



Quantitative determination of carbon nanodots in processed foods using HPLC-SEC with fluorescence detection

József Prokisch^a, Duyen H.H. Nguyen^{a,b,c,*}, Arjun Muthu^{a,d}, János Posta^e, Aron Béni^d

^a Institute of Animal Science, Biotechnology and Nature Conservation, Faculty of Agricultural and Food Sciences and Environmental Management, University of Debrecen, Böszörményi Street 138, 4032 Debrecen, Hungary

^b Doctoral School of Nutrition and Food Science, University of Debrecen, Debrecen 4032, Hungary

^c Institute of Life Sciences, Vietnam Academy of Science and Technology, 9/621 Vo Nguyen Giap Street, Linh Trung Ward, Thu Duc City 700000, Ho Chi Minh, Viet Nam

^d Institute of Agricultural Chemistry and Soil Science, Faculty of Agricultural and Food Sciences and Environmental Management, University of Debrecen, 138 Böszörményi Street, 4032 Debrecen, Hungary

^e Health Care Service Units, Diagnostic Units, Forensic Medicine, University of Debrecen Clinical Center, University of Debrecen, Nagyerdei körút 98, 4032 Debrecen, Hungary

ARTICLE INFO

Keywords:

Carbon dots
Nanomaterial quantification
Processed foods
Food nanomaterials

ABSTRACT

This study presents a validated analytical method using high-performance liquid chromatography with size exclusion and fluorescence detection (HPLC-SEC-FLD) for the quantitative determination of fluorescent carbon nanodots (CNDs) in processed foods. Addressing the lack of reliable quantitative tools in this emerging field, the method demonstrates high sensitivity (LOD: 0.080 mg/L), excellent linearity ($R^2 > 0.9993$), and strong reproducibility (RSD < 2.2%) across diverse food matrices. The morphology, crystallinity, carbon structure, and surface functional groups of the glycine-sugar-derived CND standard (Gly-CSNDs) were characterized using TEM, XRD, Raman spectroscopy, and FTIR. A glycine-sugar-derived CNDs (Gly-CSND) standard was employed for calibration, enabling accurate quantification of CNDs in samples such as coffee, darkened fruits, and caramelized products. The method showed recovery rates of 98.5–101.2% in spiked samples and consistent results across laboratories, confirming its robustness. This platform offers a specific, precise, and scalable solution for assessing CNDs content in complex food systems. It supports future research into CNDs formation during food processing and their potential health implications, laying a foundation for regulatory monitoring and safety evaluation of nanomaterials in the food supply.

1. Introduction

Carbon nanodots (CNDs) have gained significant interest in food science and materials research due to their unique photoluminescent properties, biocompatibility, and versatile synthesis routes [1,2]. CNDs are mainly composed of carbon, nitrogen, oxygen, and occasionally doped with other heteroatoms which are unintentionally formed during thermal processing of foods [3] or intentionally synthesized for applications in sensing, packaging [4] and nutritional enhancement [5,6]. They have also been used in a wide range of fields, from improving food quality [7,8] to serving as biomarkers and antimicrobial agents [9,10]. Despite gaining more attention, most investigations into CNDs have been limited to structural and optical characterization using techniques such as fluorescence spectroscopy [11–13], Raman spectroscopy [14],

Fourier-Transform Infrared spectroscopy (FTIR) [15], and transmission electron microscopy (TEM). These methods offer critical qualitative insights into surface functionality and morphology but provide less information, enabling robust quantitative determination, especially in complex matrices like processed foods [16,17]. The lack of analytical strategies to quantify CNDs content poses a potential challenge in food safety assessment, consumer awareness, and regulatory compliance. Conventionally, a fluorescence-based method has been used, which can also be limited by matrix effects. Fluorescent molecules in food can mimic the emission signals of CNDs, resulting in significant positive error in the measurements [18]. Similarly, Raman spectroscopy and TEM can offer structural information; they are inherently non-quantitative and not suitable for routine food analysis due to sample preparation complexity and limited throughput. High background

* Corresponding author at: Institute of Animal Science, Biotechnology and Nature Conservation, Faculty of Agricultural and Food Sciences and Environmental Management, University of Debrecen, Böszörményi Street 138, 4032 Debrecen, Hungary.

E-mail address: nguyen.huu.huong.duyen@agri.unideb.hu (D.H.H. Nguyen).

<https://doi.org/10.1016/j.microc.2026.117773>

Received 29 September 2025; Received in revised form 17 March 2026; Accepted 18 March 2026

Available online 19 March 2026

0026-265X/© 2026 The Authors. Published by Elsevier B.V. This is an open access article under the CC BY license (<http://creativecommons.org/licenses/by/4.0/>).

fluorescence signal from CNDs can also provide a potential background noise signal [19].

Only a few studies have attempted to fractionate CNDs. Reports including the separation of CNDs using polyacrylamide gel electrophoresis [20], capillary electrophoresis [21], and anion-exchange ion chromatography [22,23]. However, each of these approaches has notable limitations. Gel electrophoresis suffers from low separation efficiency; capillary electrophoresis, despite offering excellent resolution, yields fractions too small for comprehensive downstream characterization; and anion-exchange ion chromatography requires costly columns, pH-dependent elution conditions, and additional desalting steps prior to further analysis. Moreover, AEIC can only fractionate charged CNDs, leaving neutral species unresolved [24].

Currently, no validated analytical approach has been established for quantifying the concentration of CNDs in food systems. This represents a critical knowledge gap, especially considering the increasing prevalence of CNDs in heat-processed and functional foods [25]. These constraints highlight the urgent need for alternative, scalable, and matrix-compatible analytical separation techniques capable of resolving and quantifying CNDs in complex systems. In this context, high-performance liquid chromatography combined with size exclusion chromatography (HPLC-SEC) offers a powerful, underexplored platform. By separating nanoparticles on the basis of hydrodynamic volume rather than charge, HPLC-SEC can overcome many of the limitations of electrophoretic and ion-exchange approaches, while coupling with fluorescence detection enables sensitive and selective quantification of CNDs in real-world food matrices. Given the growing legal framework concerns over nanomaterials in consumer products, it is essential to develop accurate, reproducible, and scalable methods to detect and measure CNDs in food samples [7].

In this study, we propose a novel application of high-performance liquid chromatography coupled with size exclusion chromatography and fluorescence detection (HPLC-SEC-FLD) as a quantitative analytical platform for measuring carbon nanodots in processed food matrices. The method offers size-based separation to reduce interference from low-molecular-weight fluorophores, enabling more selective and accurate quantification. To our knowledge, this is the first demonstration of using HPLC-SEC-FLD for this purpose, offering a much-needed analytical advancement that bridges nanotechnology and food chemistry.

2. Materials and methods

2.1. HPLC-SEC-FLD system and chromatographic conditions

Quantification of carbon nanodots (CNDs) in food matrices was achieved using a high-performance liquid chromatography system coupled with size exclusion chromatography and fluorescence detection (HPLC-SEC-FLD). The chromatography system (Ecom Spol. s.r.o., Prague, Czech Republic) was optimized for nanoparticle separation. For the mobile phase, deionized water was used to elute water-soluble CNDs, while a 20% (v/v) acetonitrile solution in deionized water was employed to minimize hydrophobic interactions for other CND types.

Analyses were conducted under isocratic conditions at a flow rate of 0.7 mL/min, with an injection volume of 5 μ L. Fluorescence detection was carried out using a Shimadzu RF-20A detector set at 380 nm excitation and 460 nm emission wavelengths. Parameters were optimized using 3D fluorescence spectra to maximize sensitivity and reproducibility across different processed food matrices.

2.2. Preparation of CNDs standards and food samples

2.2.1. Carbon nanodots (CNDs) standards

Commercial CND standards synthesized from amino acid-based precursors were acquired from VWR (Debrecen, Hungary) and produced by Nanofood Laboratory, University of Debrecen. Four CND variants were used: glycine-citric acid CNDs (Gly-CNDs), glycine-sugar CNDs

(Gly-CSNDs, glucose as the sugar precursor), lysine-citric acid CNDs (Lys-CNDs), and urea-citric acid CNDs (U-CNDs). For each formulation, precursor 1 (glycine/lysine/urea) and precursor 2 (citric acid or glucose) were mixed at a 4:1 (w/w) ratio and heated by pyrolysis at 180 °C for 2 h in an oven under a closed system. The obtained powders were ground and dispersed in ultrapure water. The water-soluble fractions were collected, dialyzed overnight using a dialysis membrane (DEGASA Co., Heidelberg, Germany), freeze-dried, ground into fine powders, and stored for future use.

2.2.2. Food samples

Processed food samples were air-dried and homogenized. One gram of each sample was extracted in 100 mL of deionized water at room temperature for 2 h. Extracts were sequentially filtered through coarse (Whatman Z696145) and fine (Whatman Z240087) filter papers (Merck, Budapest, Hungary), followed by a 0.2 μ m syringe filter (Merck 41104922) prior to HPLC injection.

2.3. Chromatographic evaluation and quantification

CNDs were identified based on retention time, with peaks eluting before 10 min attributed to nanoparticle-sized species. Later-eluting peaks were assigned to smaller fluorescent molecules. Approximate molecular weights were inferred from SEC calibration curves; for example, Gly-CSNDs exhibited an estimated molecular weight of ~800 kDa and particle size of ~6.6 nm, validated by transmission electron microscopy. Quantification was based on peak area or height, calibrated using Gly-CSNDs as the reference. Results were expressed in Gly-CSNDs equivalents to enable consistent cross-sample comparisons.

2.4. Chemicals and reagents

All chemicals used were analytical grade. HPLC-grade deionized water and acetonitrile were procured from VWR (Debrecen, Hungary). All CNDs standards originated from the same supplier.

2.5. Method validation

2.5.1. Limit of detection

The detection limit was defined as the concentration producing a signal three times greater than the standard deviation of seven replicate blank analyses. Calculations used peak height values at relevant retention times, with the detection threshold determined via calibration curves.

2.5.2. Dynamic range

Calibration with Gly-CSNDs standards showed linearity from the detection limit to 10,000 mg/kg. Linearity was verified through regression analysis.

2.5.3. Reproducibility

An inter-laboratory validation was conducted at the Central Laboratory of the University of Debrecen. Using an independent analyst and instrument, Gly-CSNDs standards were reanalyzed. Results were statistically compared using ANOVA to assess method robustness.

2.5.4. Standard addition and recovery

To evaluate matrix interference and recovery, a coffee extract was spiked with Gly-CSND. Recovery was determined from the difference in concentrations before and after spiking, confirming the method's suitability for complex food matrices.

3. Results

3.1. Characterization of synthesized carbon nanodots

Four types of carbon nanodots (CNDs) were synthesized using distinct nitrogen-containing precursors combined with citric acid or glucose: glycine–citric acid (Gly-CNDs), glycine–glucose (Gly-CSNDs), urea–citric acid (U-CNDs), and lysine–citric acid (Lys-CNDs). The

lyophilized CNDs exhibited varying visual appearances depending on precursor composition (Fig. 1). Gly-CSNDs appeared brownish, Gly-CNDs were greenish-yellow, U-CNDs dark brown, and Lys-CNDs pale yellow—indicating differences in surface chemistry and carbonization degree.

To evaluate their optical characteristics, fluorescence emission spectra were recorded across multiple excitation wavelengths (300–480 nm), and excitation–emission matrices (EEMs) were generated (Fig. 1).

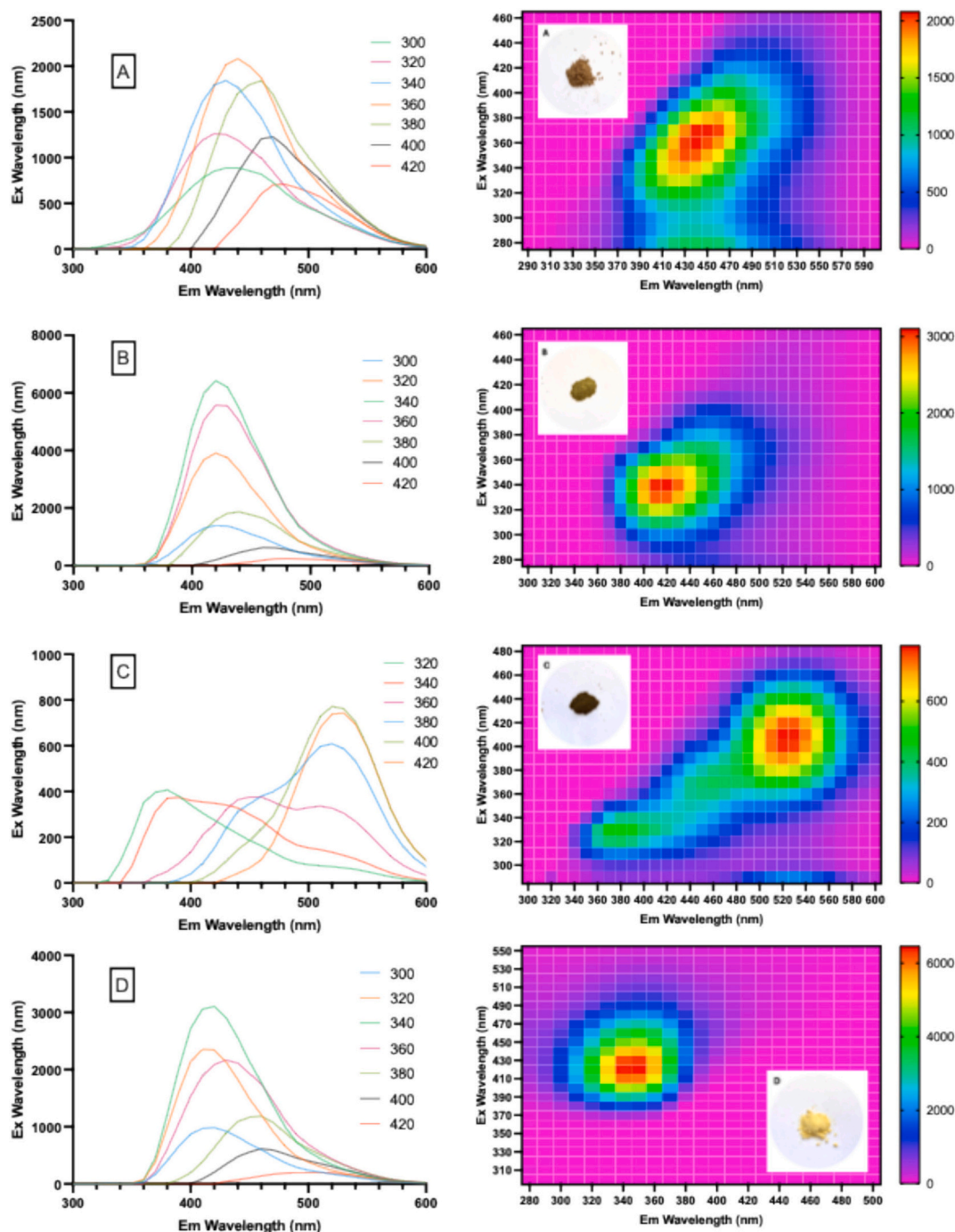


Fig. 1. Visual appearance and fluorescence characteristics of synthesized carbon nanodots (CNDs). (A–D) Four CND types synthesized from different precursors: (A) glycine–sugar-based carbon nanodots (Gly-CSNDs), (B) glycine–citric acid-based carbon nanodots (Gly-CNDs), (C) urea–citric acid-based carbon nanodots (U-CNDs), and (D) lysine–citric acid-based carbon nanodots (Lys-CNDs). Fluorescence emission spectra (left panels) and excitation–emission matrix (EEM) heatmaps (right panels) are shown for each CND type. Emission spectra were recorded at multiple excitation wavelengths (300–480 nm), while EEMs were generated by scanning excitation from 300 to 500 nm and emission from 350 to 600 nm. Photographs of the corresponding lyophilized CND powders are displayed in the corner of each heatmap. Differences in spectral profiles reflect the influence of precursor composition on surface states and fluorescence heterogeneity. These standards were used for calibration and comparative quantification in food matrix analyses.

All CND types demonstrated excitation-dependent fluorescence, a hallmark of heterogeneous surface states typical of CNDs.

Gly-CSNDs exhibited a broad emission band centered at ~ 460 nm with a maximum excitation around 360 nm, reflecting a more homogeneous emissive environment. Gly-CNDs and Lys-CNDs both showed narrower emission peaks (around 440–450 nm), with optimal excitation occurring at 340 nm. This suggests stronger quantum confinement and fewer surface defects. In contrast, U-CNDs presented dual emission features with broader intensity distribution and a less-defined excitation maximum, indicative of diverse trap states.

The EEM plots further supported these observations: Gly-CSNDs and Gly-CNDs showed distinct, localized fluorescence hotspots; U-CNDs exhibited a more diffuse pattern; and Lys-CNDs produced a single, sharp emission cluster, suggesting stable and uniform optical behavior. Collectively, these findings highlight how precursor composition and synthesis strategy influence the photoluminescent behavior of CNDs, which is essential for their use in standardized quantification or fluorescence-based sensing in complex food systems.

3.2. Development of HPLC-SEC-FLD method

A robust and reproducible analytical platform was developed using high-performance liquid chromatography coupled with size exclusion chromatography and fluorescence detection (HPLC-SEC-FLD) to quantify carbon nanodots (CNDs) in complex food matrices (Fig. 2) shows the representative chromatographic profiles of the four synthesized CNDs standards: Gly-CSNDs, Gly-CNDs, U-CNDs, and Lys-CNDs.

All samples exhibited dominant early-eluting peaks within a retention time range of 5 to 10 min, indicative of high molecular weight species. Based on the SEC column calibration, this elution window corresponds to an approximate molecular weight range of 200,000–1,000,000 Da, which is consistent with the nanoscale size of CND aggregates or individual particles. The sharpness or broadness of these peaks reflects differences in hydrodynamic diameter and polydispersity. For example, Gly-CNDs produced a sharp and intense peak, suggesting a relatively uniform particle population, whereas U-CNDs and Lys-CNDs displayed broader peaks, indicating more heterogeneous distributions. These differences in retention behavior also highlight variations in surface chemistry and molecular interactions with the stationary phase, influenced by the nitrogen-containing precursors used in synthesis. Late-eluting secondary peaks were also observed in all samples, attributed to lower molecular weight fluorescent fragments or degradation products.

The TEM image (Fig. 3A) reveals that the synthesized Gly-CSNDs are well-dispersed and predominantly quasi-spherical in morphology, with no significant aggregation observed. The average particle size calculated from multiple TEM measurements (Fig. 3B) falls within the typical CNDs range (<10 nm), confirming successful nanoscale formation. The relatively narrow Gaussian distribution suggests a controlled nucleation and carbonization process during synthesis, likely governed by Maillard-type reactions between glycine and glucose. FTIR spectra (Fig. 3C) demonstrate clear chemical transformation from precursors to CNDs. While glycine and glucose exhibit characteristic bands corresponding to $-\text{NH}_2$, $-\text{OH}$, and $\text{C}=\text{O}$ functional groups, the Gly-CSNDs retain broad $\text{O}-\text{H}/\text{N}-\text{H}$ stretching bands (~ 3200 – 3500 cm^{-1}), $\text{C}=\text{O}$ stretching (~ 1650 – 1720 cm^{-1}), and $\text{C}-\text{N}/\text{C}-\text{O}$ vibrations (~ 1000 – 1400 cm^{-1}). The persistence of oxygen- and nitrogen-containing functional groups indicates incomplete carbonization and abundant surface passivation, which is typical for CNDs synthesized via bottom-up thermal routes. These surface functionalities are crucial for aqueous dispersibility and potential bioactivity. The Raman spectrum (Fig. 3D) shows two prominent peaks corresponding to the D band (~ 1350 cm^{-1}) and G band (~ 1580 cm^{-1}), attributed to disordered sp^2 carbon and graphitic sp^2 domains, respectively. The intensity ratio ($I_{\text{D}}/I_{\text{G}}$) suggests a predominantly amorphous or nanocrystalline carbon structure with small sp^2 clusters embedded in an sp^3 matrix, consistent with typical CNDs

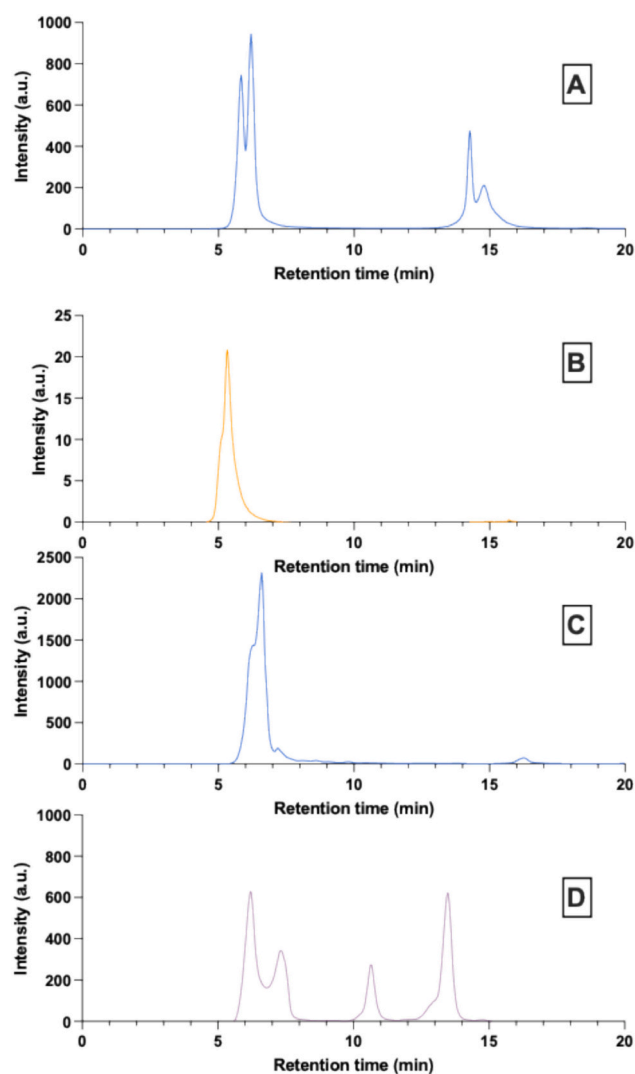


Fig. 2. HPLC-SEC-FLD chromatograms of synthesized carbon nanodots (CNDs). Representative size exclusion chromatograms with fluorescence detection (Ex/Em: 380/460 nm) for: (A) glycine-glucose carbon nanodots (Gly-CSNDs), (B) glycine-citric acid carbon nanodots (Gly-CNDs), (C) urea-citric acid carbon nanodots (U-CNDs), and (D) lysine-citric acid nanodots (Lys-CNDs). Each chromatogram displays characteristic retention time profiles corresponding to the nanoparticulate fraction (early-eluting peaks) and smaller fluorescent species (late-eluting peaks). Peak positions and intensities indicate differences in hydrodynamic size distribution and fluorescent yield among CND types.

derived from organic precursors. The XRD pattern (Fig. 3E) displays a broad diffraction peak centered around $2\theta \approx 20$ – 25° , characteristic of amorphous carbon with turbostratic structure. The absence of sharp crystalline peaks confirms the lack of long-range order. The SAED inset further supports this observation, showing diffuse concentric rings rather than discrete diffraction spots, indicative of polycrystalline or amorphous carbon domains.

Collectively, the structural and chemical characterization results (Fig. 3) confirm the successful synthesis of nanosized, amorphous, nitrogen-containing CNDs with abundant surface functional groups derived from glycine and glucose. The quasi-spherical morphology, narrow size distribution, disordered sp^2/sp^3 carbon structure, and oxygen-/nitrogen-rich surface chemistry are consistent with typical Maillard-derived CNDs formed in thermally processed foods. In combination with the well-defined fluorescence properties demonstrated in Fig. 1, Gly-CSNDs exhibit strong, reproducible emission behavior and good dispersibility in aqueous media. These features are essential for

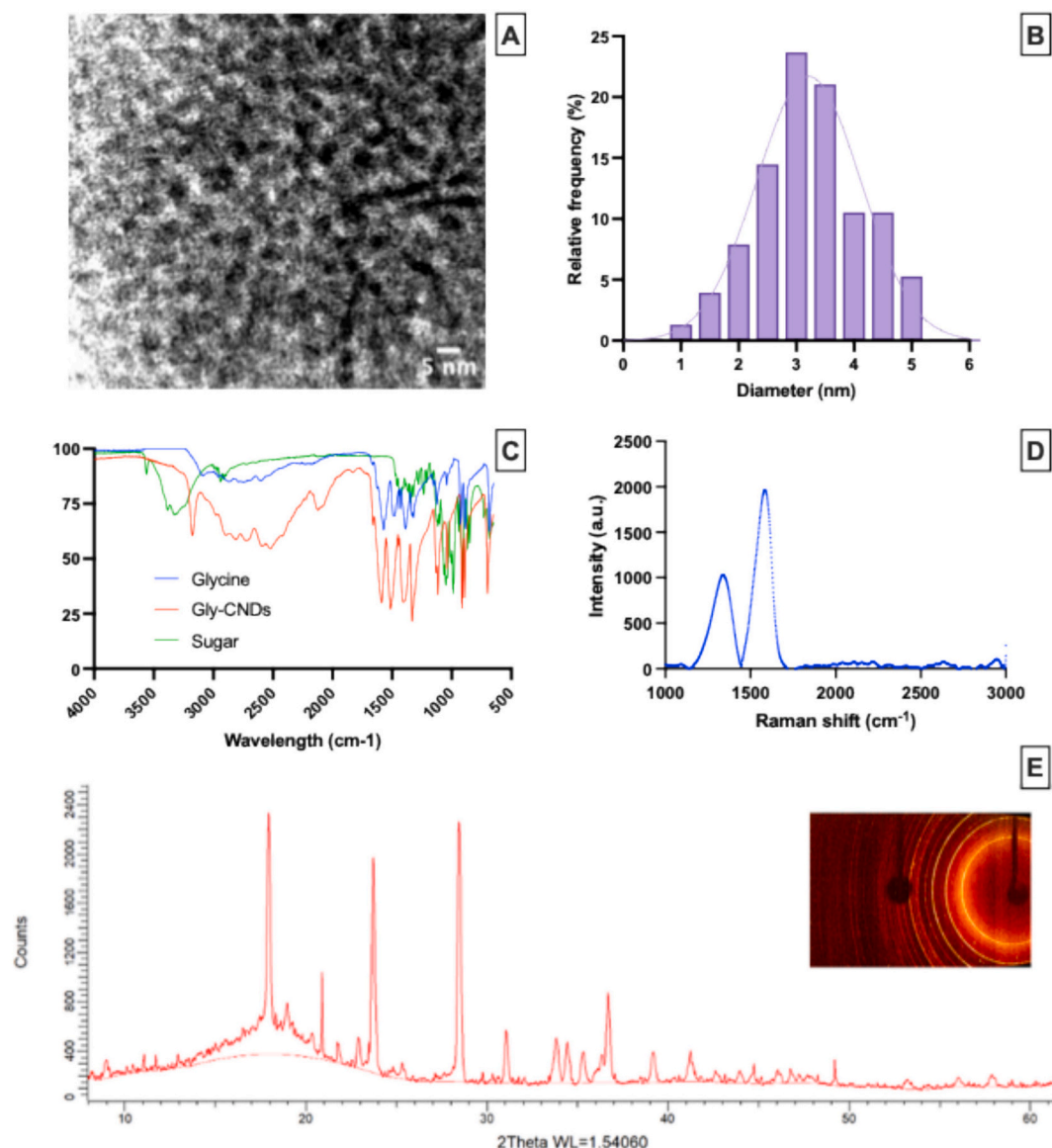


Fig. 3. Characterization of glycine–glucose carbon nanodots (Gly-CSNDs). (A) Transmission electron microscopy (TEM) image showing quasi-spherical nanoparticles with uniform dispersion. Scale bar: 5 nm. (B) Particle size distribution histogram derived from TEM images, fitted with a Gaussian distribution. (C) Fourier transform infrared (FTIR) spectra of glycine, glucose, and synthesized Gly-CSNDs. (D) Raman spectrum of Gly-CSNDs showing characteristic D and G bands. (E) X-ray diffraction (XRD) pattern of Gly-CSNDs; inset shows the corresponding selected area electron diffraction (SAED) pattern.

chromatographic detection based on fluorescence response. Therefore, Gly-CSNDs were considered an appropriate and representative standard material for the development of the HPLC-SEC-FD method aimed at detecting and quantifying carbon nanodots in complex food matrices.

For quantitative calibration, Gly-CSNDs were selected due to their stability and consistent fluorescent response. Fig. 4A illustrates the dose-dependent fluorescence chromatograms of Gly-CSNDs across a concentration range of 5–200 mg/L. The resulting calibration curve (Fig. 4B) exhibited excellent linearity on the range of 0–10,000 mg/L with $R^2 > 0.9993$, supporting the method's reliability for quantification. The limit of detection (LOD) was determined to be 0.080 mg/L, and the limit of quantification (LOQ) was 0.243 mg/L, indicating high sensitivity suitable for trace-level detection of CNDs in processed foods. These values were established through seven replicate blank measurements and $3.3\sigma/10\sigma$ signal threshold calculations. The chromatographic and analytical performance demonstrated by this method positions it as a practical tool for routine screening of nanoparticulate carbon species in food products, with potential adaptability for other carbon-based nanomaterials.

3.3. Method validation

3.3.1. Linearity and calibration

The calibration curve for Gly-CSNDs was previously described in Section 3.2. The method exhibited excellent linearity across the range of 0–10,000 mg/L, with an $R^2 > 0.9993$. These results confirm the suitability of the method for quantitative analysis.

3.3.2. Detection and quantification limits (LOD/LOQ)

As reported in Section 3.2, the LOD and LOQ were determined to be 0.080 mg/L and 0.243 mg/L, respectively, based on a $3.3\sigma/10\sigma$ approach from blank replicates. These values confirm the method's sensitivity for trace-level detection of CNDs in processed food matrices.

3.3.3. Precision and repeatability (intra/inter-day %RSD)

To evaluate inter-laboratory reproducibility, the complete analytical protocol for HPLC-SEC-FLD was transferred to an independent laboratory (Lab B), where Gly-CSND standards were reanalyzed using

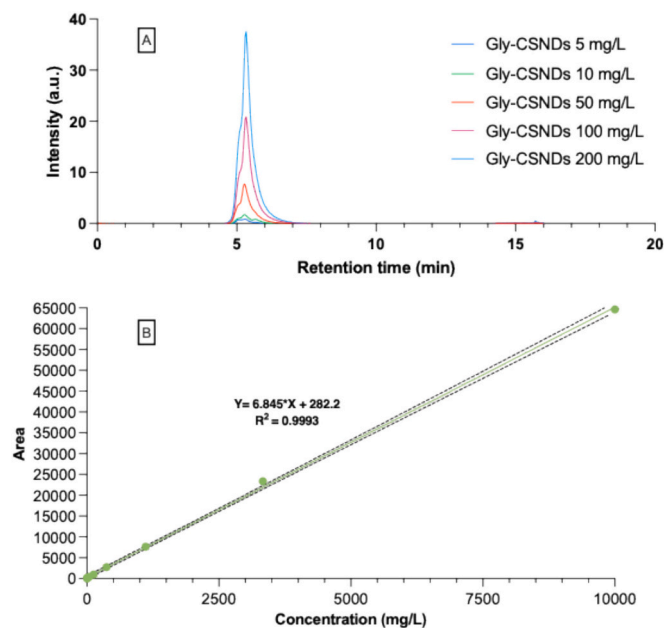


Fig. 4. Calibration of HPLC-SEC-FLD method using Gly-CSND standards. (A) Fluorescence chromatograms of Gly-CSNDs at varying concentrations (5–200 mg/L) show consistent retention time and proportional increase in peak intensity. (B) Calibration curve constructed from peak area vs. concentration of Gly-CSNDs, demonstrating excellent linearity across the tested range (0–10,000 mg/L). The method yielded a limit of detection (LOD) of 0.080 mg/L and a limit of quantification (LOQ) of 0.243 mg/L.

equivalent instrumentation. Fig. 5A presents an overlay of chromatograms generated by both laboratories. Despite minor retention time shifts—likely resulting from variations in system dead volume or column batch—both chromatograms exhibited identical elution profiles and comparable peak intensities.

Table 1 summarizes the retention times (RT), CND concentrations, and associated relative standard deviations (%RSD) for two standard concentrations (100 and 200 mg/L) measured in both labs. Across both laboratories, RT values showed excellent consistency, with <0.5% deviation, confirming robust chromatographic separation. Quantitative measurements of CNDs concentrations were also highly comparable, with RSD values for intra-lab repeatability below 4% in both settings.

These findings underscore the robustness, repeatability, and inter-laboratory transferability of the method. The observed consistency between laboratories confirms the method's reliability for standardized implementation in multi-center studies, routine quality control, and regulatory surveillance. Additionally, the low %RSD across independent replicates highlights the method's potential for international harmonization of CND quantification workflows.

3.3.4. Accuracy and recovery (spiked samples)

To evaluate the accuracy of the HPLC-SEC-FLD method and assess potential matrix effects, a recovery experiment was performed using coffee extract as a representative complex food matrix. The extract was spiked with glycine-sugar-derived carbon nanodots (Gly-CSNDs) at varying concentrations ranging from 5 to 200 mg/L. As summarized in Table 2 and Fig. 5B, the measured concentrations closely matched the theoretical spiking levels, yielding recovery rates between 98.51% and 101.20%. The method also demonstrated excellent repeatability, with relative standard deviations (RSD%) below 2.2% for all tested concentrations ($n = 3$). These results confirm the method's robustness, minimal matrix interference, and its strong suitability for accurate quantification of CNDs in real food matrices such as coffee. The consistent retention time and absence of co-eluting peaks further underscore the analytical specificity and reliability of the HPLC-SEC-FLD system for spiked

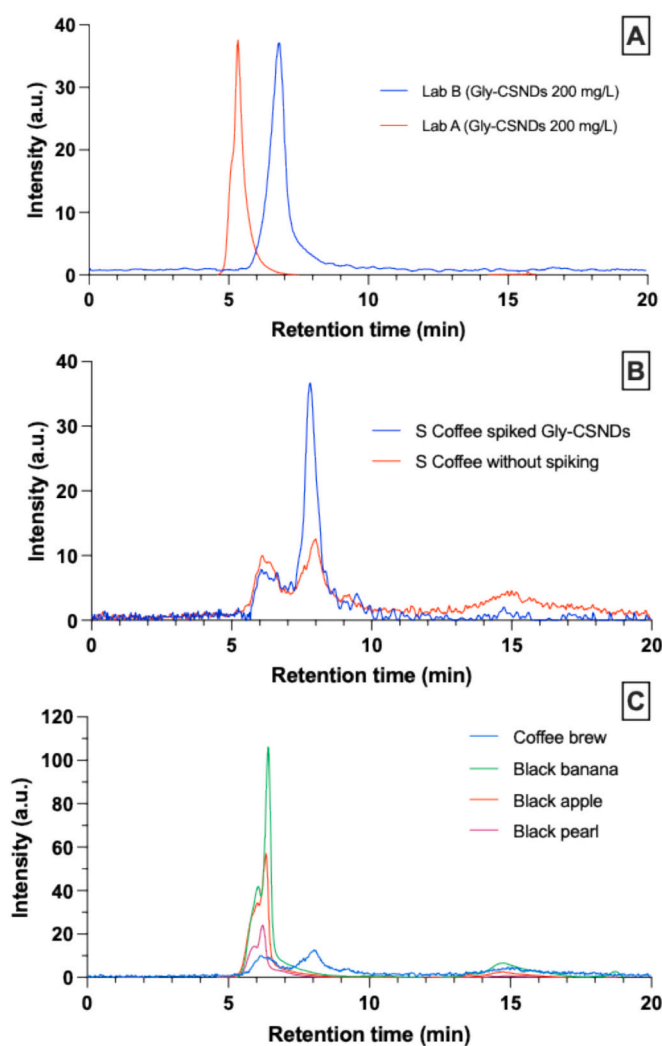


Fig. 5. HPLC-SEC-FLD chromatograms of Gly-CSNDs and selected processed food samples. (A) Inter-laboratory comparison of Gly-CSND chromatograms obtained in two independent laboratories using different instruments and analysts. (B) Chromatograms of coffee extract without spiking (red) and after spiking with Gly-CSNDs at 1 mg/L (blue), showing enhanced fluorescence at the characteristic retention time (~3.5–4.0 min). (C) Overlaid chromatograms of carbon nanodots detected in coffee brew, black banana, black apple, and black pearl beverage. All samples were analyzed using the validated HPLC-SEC-FLD method and quantified against Gly-CSND calibration standards. (For interpretation of the references to colour in this figure legend, the reader is referred to the web version of this article.)

recovery applications.

3.3.5. Summary table of validation metrics

A comprehensive summary of the method validation parameters for the HPLC-SEC-FLD quantification of carbon nanodots (CNDs) is summarized. The method exhibited excellent linearity ($R^2 > 0.9993$) over a wide dynamic range (0–10,000 mg/L), confirming its suitability for detecting CNDs in diverse food matrices. The limit of detection (LOD) and limit of quantification (LOQ) were calculated as 0.080 mg/L and 0.243 mg/L, respectively, enabling sensitive detection even at trace levels. Accuracy was demonstrated through spiking experiments, with recoveries ranging from 98.5% to 101.2%, and RSD values consistently below 2.2%. Intra-day precision (repeatability) was below 3%, while inter-day precision and inter-laboratory reproducibility both remained under 5%, as validated by independent testing across laboratories using the same analytical protocol. Retention times remained stable, and

Table 1
Inter-laboratory Comparison of HPLC-SEC-FLD Performance: Retention Time and Quantification of Gly-CSND Standards at Two Concentrations.

Gly-CSNDs (mg/L)	Retention time, R_T (min)				CNDs (mg/L)			
	Lab A		Lab B		Lab A		Lab B	
	Mean	RSD (%)	Mean	RSD (%)	Mean	RSD (%)	Mean	RSD (%)
100	5.32 ± 0.02 ^b	0.36	6.81 ± 0.02 ^a	0.28	6.16 ± 0.24 ^A	3.9	6.4 ± 0.23 ^A	3.56
200	5.32 ± 0.02 ^b	0.36	6.8 ± 0.03 ^a	0.49	11.98 ± 0.23 ^B	1.91	12.21 ± 0.23 ^B	1.91

Values are expressed as mean ± standard deviation ($n = 3$). RSD: relative standard deviation. Superscript letters a, b within the same row denotes statistically significant differences in retention time between laboratories ($p < 0.001$). Superscript capital letters A, B indicate statistically significant differences in CND concentrations across spiking levels ($p < 0.001$, one-way ANOVA with Tukey's post hoc test). No significant differences were observed between laboratories for CND concentrations at the same spiking level ($p > 0.001$).

Table 2
Recovery of Gly-CSNDs in coffee extract at varying spiking concentrations, demonstrating method accuracy and precision.

Added Gly-CSNDs concentration (mg/L)	Measured Concentration (mg/L)	Recovery (%)	RSD (%)	n
0	93.19 ± 0.32	100	0.34	3
5	129.79 ± 0.15	100.66 ± 0.1	0.12	3
		101.2 ± 1.79		
10	135.69 ± 2.87	98.67 ± 1.06	2.12	3
		98.51 ± 0.85		
50	171.1 ± 2.13	98.73 ± 0.57	1.24	3
		1.06		
100	220.03 ± 2.12	0.85	0.96	3
		98.73 ± 0.57		
200	319.3 ± 2.01	0.57	0.63	3

chromatographic profiles were consistent, supporting the robustness and transferability of the method. These results collectively confirm that the HPLC-SEC-FLD method is highly accurate, precise, and reproducible, meeting the analytical requirements for routine application in research, quality control, and regulatory monitoring of food-derived carbon nanodots.

3.4. Application to real samples

The validated HPLC-SEC-FLD method was applied to various processed food products known for intense thermal or oxidative treatments, including coffee, black banana, black apple, and black pearl drink. As shown in Fig. 5C, all samples exhibited pronounced fluorescence peaks corresponding to the expected retention time range of Gly-CSNDs (approximately 5.3–5.6 min), confirming the presence of CNDs within these complex food matrices. Distinct differences in peak intensity and width were observed among the food samples, reflecting variability in CND concentration and possibly differences in nanoparticle size distribution or surface chemistry. Notably, black banana and black apple showed the highest peak intensities, indicating a greater accumulation of CNDs. This aligns with expectations, as these fruits undergo extensive enzymatic browning and sugar-rich Maillard reactions during over-ripening and darkening.

Table 3
Concentration of CNDs in different food samples expressed in Gly-CSND equivalent.

Samples	CNDs content (mg/L Gly-CSNDs equivalent)
Coffee brew	384.97 ± 13.14 ^c
Black banana	977.75 ± 16.24 ^a
Black apple	655.14 ± 8.13 ^b
Black pearl	270.53 ± 11.7 ^d

Values are presented as mean ± standard deviation ($n = 3$). Different superscript letters (a–d) indicate statistically significant differences among samples ($p < 0.001$, one-way ANOVA followed by Tukey's post hoc test).

Quantitative results summarized in Table 3 support the chromatographic findings. Black banana exhibited the highest CNDs content at 977.75 ± 16.24 mg/L, followed by black apple (655.14 ± 8.13 mg/L) and coffee brew (384.97 ± 13.14 mg/L). The black pearl beverage, a commercial sweetened drink, contained the lowest concentration (270.53 ± 11.7 mg/L), suggesting a different formation pathway or dilution effect. These results indicate that both thermal processing (as in coffee and toasted grains) and natural oxidation or enzymatic degradation (as in fruits) significantly contribute to in situ CND formation. The method's ability to resolve and quantify these nanostructures with high precision across diverse matrices highlights its applicability for dietary exposure assessment and quality monitoring of processed foods.

3.5. Comparative analysis with other methods

Numerous analytical techniques have been employed to detect and quantify carbon nanodots (CNDs), including UV-Vis and fluorescence spectroscopy, Raman spectroscopy, transmission electron microscopy (TEM), and various chromatography-based methods. While each approach has specific applications, their limitations become evident in complex matrices such as processed foods. Table 4 compares the analytical methods for Carbon Nanodot (CND) Quantification.

UV-Vis and fluorescence spectroscopy are commonly used for rapid screening and characterization of CNDs. However, their lack of molecular separation leads to signal overlap and matrix interference, significantly reducing specificity in complex samples [18,26,27]. This restricts their utility in quantitative applications, especially when precision and selectivity are critical.

Raman spectroscopy, although useful for structural fingerprinting, is compromised by the intrinsic fluorescence of CNDs and food components, which often overwhelms the Raman signal. These fluorescence interferences, combined with low quantification reliability, limit Raman's effectiveness in CND analysis [26,27].

Transmission electron microscopy (TEM) provides high-resolution imagery for assessing particle morphology and size distribution, making it valuable for fundamental characterization. However, TEM is qualitative, low-throughput, and requires extensive sample preparation, rendering it impractical for routine analysis in food matrices [22,24,28]. Other chromatographic methods, including reverse-phase HPLC (RP-HPLC) and anion-exchange HPLC (AE-HPLC), offer better resolution than spectroscopic techniques but still fall short in complex food systems. These approaches often necessitate intensive sample cleanup and lack broad validation for food-based quantification [22,28]. Quantitative performance metrics such as reproducibility and detection limits are also rarely reported.

In contrast, the HPLC-SEC-FLD method developed in this study provides a robust and highly sensitive platform tailored for the quantification of CNDs in complex food matrices. It enables both size-based separation and fluorescence-based detection, mitigating matrix interference while allowing for precise nanoparticle quantification. As reported by Trubetskaya et al. (2021), this method demonstrates high reproducibility ($\leq 3\%$ deviation) and effectively isolates CND fractions from non-fluorescent and low-molecular-weight impurities [29]. These

Table 4
Comparative Analysis of Analytical Methods for Carbon Nanodot (CND) Quantification.

Method	LOD/LOQ	Advantages	Disadvantages	Ref.
HPLC-SEC-FLD (This study)	LOD: 0.068 mg/L LOQ: 0.206 mg/L	High specificity, size-based separation, suitable for complex food matrices, reproducible across labs (RSD < 2.2%)	Requires FLD detector and SEC optimization; moderate instrumentation cost	This study
UV-Vis / Fluorescence Spectroscopy	Not consistently reported	Rapid screening, accessible instrumentation	Low specificity, overlapping signals in complex samples	[18,26,27]
Raman Spectroscopy	Not applicable	Structural fingerprinting, non-destructive	Fluorescence interference, low quantification reliability	[26,27]
Transmission Electron Microscopy (TEM)	Not applicable	High-resolution imaging, particle morphology	Qualitative only, low throughput, complex prep	[24] [28] [22]
RP-HPLC	Not reported	Some separation capability, applicable to synthetic CNDs	Limited data in food matrices, requires secondary validation	[28] [24]
AE-HPLC	Not reported	Selective for charged species, some environmental applications	Matrix complexity requires extensive prep	[22].
LC-MS	LOD: 0.002–0.005% w/w (LC-UV); 0.04–1.1 µg/g (LC-APCI-MS); 0.4 pg/L–1.6 ng/L (LC-APPI-MS)	Ultra-sensitive, detailed molecular info	High cost, requires standards, complex operation	[26]

characteristics make it especially well-suited for processed food applications where matrix complexity is a significant analytical barrier.

In summary, while traditional methods serve important roles in characterizing CNDs, HPLC-SEC-FLD offers the most practical balance of specificity, sensitivity, and reproducibility for quantitative analysis in food systems. Its adaptability, coupled with the ability to analyze multiple CND types simultaneously, underscores its potential as a standard method for CND monitoring in food safety, nanotoxicology, and regulatory frameworks.

4. Future perspectives

The validated HPLC-SEC-FLD method demonstrated excellent performance for quantifying carbon nanodots (CNDs) in diverse processed food matrices, with high sensitivity (LOD: 0.068 mg/L) and robust reproducibility (RSD < 2.2%). Its success highlights future opportunities for both research and regulatory applications. Further investigations should focus on the formation mechanisms of CNDs during high-heat processing, especially via Maillard reactions and caramelization. Real-world food systems and model reactions should be studied to identify factors influencing CND generation and accumulation. Additionally, the bioavailability and potential health impacts of food-borne CNDs remain largely unexplored. Research on their absorption, metabolic fate, and long-term biological effects is essential to inform toxicological risk assessment. Finally, standardized protocols and certified reference materials are needed to harmonize inter-laboratory results and support broader surveillance efforts. This will strengthen food safety oversight and guide best practices in food processing and formulation.

5. Conclusion

This study presents a highly sensitive and reproducible HPLC-SEC-FLD method for the quantitative determination of CNDs in processed foods. The method showed excellent linearity ($R^2 > 0.9993$), low detection limits (LOD: 0.080 mg/L, LOQ: 0.243 mg/L), and recovery rates between 98.5 and 101.2% across spiked samples. Its successful application across various food types and consistency in inter-laboratory trials demonstrate its readiness for broader deployment. Beyond analytical performance, the findings underscore the need to evaluate the formation and potential health effects of CNDs in thermally processed foods. As interest in nanomaterials and food safety grows, this method provides a crucial platform for advancing risk assessment, regulation, and transparency in the food supply.

CRediT authorship contribution statement

József Prokisch: Writing – review & editing, Supervision, Project administration, Methodology, Investigation, Funding acquisition. **Duyen H.H. Nguyen:** Writing – review & editing, Writing – original draft, Visualization, Validation, Project administration, Methodology, Formal analysis, Conceptualization. **Arjun Muthu:** Visualization, Formal analysis, Data curation. **János Posta:** Writing – review & editing, Resources, Data curation. **Aron Béni:** Writing – review & editing, Software, Formal analysis, Data curation.

Declaration of competing interest

The authors declare that they have no known competing financial interests or personal relationships that could have appeared to influence the work reported in this paper.

Acknowledgment

The authors would like to thank the Stipendium Hungaricum Scholarship program and the University of Debrecen Scientific Research Bridging Fund (DETKA). The University of Debrecen Program for Scientific Publication supports the article.

Data availability

Data will be made available on request.

References

- [1] L. Lin, X.-X. Wang, S.-Q. Lin, L.-H. Zhang, C.-Q. Lin, Z.-M. Li, J.-M. Liu, Research on the spectral properties of luminescent carbon dots, *Spectrochim. Acta A Mol. Biomol. Spectrosc.* 95 (2012) 555–561, <https://doi.org/10.1016/j.saa.2012.04.049>.
- [2] X.T. Zheng, A. Ananthanarayanan, K.Q. Luo, P. Chen, Glowing graphene quantum dots and carbon dots: properties, syntheses, and biological applications, *Small* 11 (2015) 1620–1636, <https://doi.org/10.1002/sml.201402648>.
- [3] D. Semsey, D.H.H. Nguyen, G. Törös, V. Papp, J. Péntzes, T. Vida, Á. Béni, M. Rai, J. Prokisch, Analysis of fluorescent carbon nanodots synthesized from spices through thermal processes treatment, *Nanomaterials* 15 (2025), <https://doi.org/10.3390/nano15080625>.
- [4] A. Muthu, D.H.H. Nguyen, C. Neji, G. Törös, A. Ferroudj, R. Atieh, J. Prokisch, H. El-Ramady, Á. Béni, Nanomaterials for smart and sustainable food packaging: Nano-sensing mechanisms, and regulatory perspectives, *Foods* 14 (2025), <https://doi.org/10.3390/foods14152657>.
- [5] S. Wahyudi, I. Rizoputra, C. Panatarani, F. Faizal, A. Bahtiar, Green synthesis of carbon nanodots (CNDs) moderated by flavonoid extracts from *Moringa oleifera* leaves and co-doped Sulfur/nitrogen (NS – CNDs – Fla) and their potential for heavy metals sensing application, *J. Fluoresc.* 35 (2025) 5603–5615, <https://doi.org/10.1007/s10895-024-03931-2>.

- [6] G. Törös, J. Prokisch, Maillard reaction-derived carbon nanodots: food-origin nanomaterials with emerging functional and biomedical potential, *Pharmaceutics* 17 (2025), <https://doi.org/10.3390/pharmaceutics17081050>.
- [7] D.H.H. Nguyen, A. Muthu, T. Elsakrawy, M.H. Sheta, N. Abdalla, H. El-Ramady, J. Prokisch, Carbon nanodots-based sensors: a promising tool for detecting and monitoring toxic compounds, *Nanomaterials* 15 (2025), <https://doi.org/10.3390/nano15100725>.
- [8] D.H.H. Nguyen, H. El-Ramady, J. Prokisch, Food safety aspects of carbon dots: a review, *Environ. Chem. Lett.* 23 (2025) 337–360, <https://doi.org/10.1007/s10311-024-01779-3>.
- [9] T. Chatzimitakos, C. Stalikas, Chapter 14 - Antimicrobial properties of carbon quantum dots, in: S. Rajendran, A. Mukherjee, T.A. Nguyen, C. Godugu, R. K. Shukla (Eds.), *Nanotoxicity*, Elsevier, 2020, pp. 301–315, <https://doi.org/10.1016/B978-0-12-819943-5.00014-2>.
- [10] P. Li, L. Sun, S. Xue, D. Qu, L. An, X. Wang, Z. Sun, Recent advances of carbon dots as new antimicrobial agents, *SmartMat* 3 (2022) 226–248, <https://doi.org/10.1002/smm2.1131>.
- [11] S. Li, L. Wang, C.C. Chusuei, V.M. Suarez, P.L. Blackwelder, M. Micic, J. Orbulescu, R.M. Leblanc, Nontoxic carbon dots potently inhibit human insulin fibrillation, *Chem. Mater.* 27 (2015) 1764–1771, <https://doi.org/10.1021/cm504572b>.
- [12] Y. Zhou, A. Desserre, S.K. Sharma, S. Li, M.H. Marksberry, C.C. Chusuei, P. L. Blackwelder, R.M. Leblanc, Gel-like carbon dots: characterization and their potential applications, *ChemPhysChem* 18 (2017) 890–897, <https://doi.org/10.1002/cphc.201700038>.
- [13] D. Nguyen, A. Muthu, H. El-Ramady, L. Daróczy, L. Nagy, S. Kéki, Á. Béni, I. Csarnovics, J. Prokisch, Optimization of extraction conditions to synthesize green carbon nanodots using the Maillard reaction, *Mater. Adv.* (2024), <https://doi.org/10.1039/D4MA00037D>.
- [14] K.J. Mintz, M. Bartoli, M. Rovere, Y. Zhou, S.D. Hettiarachchi, S. Paudyal, J. Chen, J.B. Domena, P.Y. Liyanage, R. Sampson, D. Khadka, R.R. Pandey, S. Huang, C. C. Chusuei, A. Tagliaferro, R.M. Leblanc, A deep investigation into the structure of carbon dots, *Carbon* 173 (2021) 433–447, <https://doi.org/10.1016/j.carbon.2020.11.017>.
- [15] H. Ding, S.-B. Yu, J.-S. Wei, H.-M. Xiong, Full-color light-emitting carbon dots with a surface-state-controlled luminescence mechanism, *ACS Nano* 10 (2016) 484–491, <https://doi.org/10.1021/acs.nano.5b05406>.
- [16] H.-W. Chu, J.-Y. Mao, C.-W. Lien, P.-H. Hsu, Y.-J. Li, J.-Y. Lai, T.-C. Chiu, C.-C. Huang, Pulse laser-induced fragmentation of carbon quantum dots: a structural analysis, *Nanoscale* 9 (2017) 18359–18367, <https://doi.org/10.1039/C7NR07639H>.
- [17] M.A. Ahmad, S. Sumarsih, J. Chang, M.Z. Fahmi, Mass spectrometry-based analyses of carbon nanodots: structural elucidation, *ACS Omega* 9 (2024) 20720–20727, <https://doi.org/10.1021/acsomega.4c01674>.
- [18] J.V. Kumar, J.-W. Rhim, Fluorescent carbon quantum dots for food contaminants detection applications, *J. Environ. Chem. Eng.* 12 (2024) 111999, <https://doi.org/10.1016/j.jece.2024.111999>.
- [19] R.R. Nigmatullin, D. Baleanu, D. Povarova, N. Salah, S.S. Habib, A. Memic, Raman spectra of Nanodiamonds: new treatment procedure directed for improved Raman signal marker detection, *Math. Probl. Eng.* 2013 (2013) 847076, <https://doi.org/10.1155/2013/847076>.
- [20] H. Liu, T. Ye, C. Mao, Fluorescent carbon nanoparticles derived from candle soot, *Angew. Chem. Int. Ed.* 46 (2007) 6473–6475, <https://doi.org/10.1002/anie.200701271>.
- [21] J.S. Baker, L.A. Colón, Influence of buffer composition on the capillary electrophoretic separation of carbon nanoparticles, *J. Chromatogr. A* 1216 (2009) 9048–9054, <https://doi.org/10.1016/j.chroma.2009.08.063>.
- [22] J.C. Vinci, L.A. Colon, Fractionation of carbon-based nanomaterials by anion-exchange HPLC, *Anal. Chem.* 84 (2012) 1178–1183, <https://doi.org/10.1021/ac202667x>.
- [23] J.C. Vinci, I.M. Ferrer, S.J. Seedhouse, A.K. Bourdon, J.M. Reynard, B.A. Foster, F. V. Bright, L.A. Colón, Hidden properties of carbon dots revealed after HPLC fractionation, *J. Phys. Chem. Lett.* 4 (2013) 239–243, <https://doi.org/10.1021/jz301911y>.
- [24] X. Gong, Q. Hu, M. Chin Paau, Y. Zhang, L. Zhang, S. Shuang, C. Dong, M.M. F. Choi, High-performance liquid chromatographic and mass spectrometric analysis of fluorescent carbon nanodots, *Talanta* 129 (2014) 529–538, <https://doi.org/10.1016/j.talanta.2014.04.008>.
- [25] D. Semsey, D.H.H. Nguyen, G. Törös, A. Muthu, S. Labidi, H. El-Ramady, Á. Béni, M. Rai, P. József, Analysis of fluorescent carbon nanodot formation during pretzel production, *Nanomaterials* 14 (2024), <https://doi.org/10.3390/nano14131142>.
- [26] A. Astefanei, O. Núñez, M.T. Galceran, Characterisation and determination of fullerenes: a critical review, *Anal. Chim. Acta* 882 (2015) 1–21, <https://doi.org/10.1016/j.aca.2015.03.025>.
- [27] B.K. John, T. Abraham, B. Mathew, A review on characterization techniques for carbon quantum dots and their applications in agrochemical residue detection, *J. Fluoresc.* 32 (2022) 449–471, <https://doi.org/10.1007/s10895-021-02852-8>.
- [28] Q. Hu, M.C. Paau, M.M.F. Choi, Y. Zhang, X. Gong, L. Zhang, Y. Liu, J. Yao, Better understanding of carbon nanoparticles via high-performance liquid chromatography-fluorescence detection and mass spectrometry, *Electrophoresis* 35 (2014) 2454–2462, <https://doi.org/10.1002/elps.201400197>.
- [29] O.E. Trubetskaya, O.A. Trubetskoj, C. Richard, A.M. Vervald, S.A. Burikov, V. V. Marchenkov, O.A. Shenderova, S.V. Patsaeva, T.A. Dolenko, High-performance size exclusion chromatography with online fluorescence and multi-wavelength absorbance detection for isolation of high-purity carbon dots fractions, free of non-fluorescent material, *J. Chromatogr. A* 1650 (2021) 462251, <https://doi.org/10.1016/j.chroma.2021.462251>.